IEEE Access
Multidisciplinary | Rapid Review | Open Access Journal

Received September 3, 2018, accepted September 27, 2018, date of publication October 22, 2018,
date of current version November 14, 2018.

Digital Object Identifier 10.1109/ACCESS.2018.2875929

An Optimal Coordinated Method for EVs Participating in Frequency Regulation Under Different Power System Operation States

CANBING LI[1,2], (Senior Member, IEEE), LONG ZENG[1,2], BIN ZHOU[1,2], (Senior Member, IEEE), XUBIN LIU[1,2], QIUWEI WU[3], (Senior Member, IEEE), DI ZHANG[1,2], (Student Member, IEEE), AND SHENG HUANG[3]

[1]Hunan Key Laboratory of Intelligent Information Analysis and Integrated Optimization for Energy Internet, Hunan University, Changsha 410082, China
[2]College of Electrical and Information Engineering, Hunan University, Changsha 410082, China
[3]Center for Electric Power and Energy, Department of Electrical Engineering, Technical University of Denmark, 2800 Kongens Lyngby, Denmark

Corresponding author: Bin Zhou (binzhou@hnu.edu.cn)

This work was supported by the Sino-U.S. International Science and Technology Cooperation Project under Grant 2016YFE0105300.

ABSTRACT This paper proposes an optimal coordinated method for electric vehicles (EVs) participating in frequency regulation (FR) under different power system operation states (PSOSs). In the proposed methodology, the FR power of EVs and generators is coordinated with different optimization objectives for power system secure and economic operations. When a power system operates in normal state, the minimum FR cost is used as an optimization objective considering the battery degradation cost. In the abnormal state, the minimum frequency restoring time is considered in the optimization objective. Based on the optimized results in different scenarios, the output power coordinated control rule between EVs and generators is drawn. Simulations on an interconnected two-area power system have validated the superiority of the proposed optimized coordinated control strategy.

INDEX TERMS Electric vehicles, frequency regulation, operation state, coordinated control, vehicle-to-grid.

I. INTRODUCTION

In order to reduce exhaust emissions and protect environment, many countries encourage renewable energy generation [1]. In the future, renewable energy sources will be massively integrated into power grids and the power system will face serious challenges. Due to the intermittency and uncertainty of renewable energy sources, it is difficult to meet the supply-demand match by only relying on the traditional FR resources [2]. EVs are considered as energy storage devices [3], [4]. Based on vehicle-to-grid (V2G) technology, EVs could charge/discharge from/to power grids [1]. The V2G power in United States, UK, Germany, Italy, etc. may reach 6.8-10 times of their average national load [5], [6], and the number of EVs in the United States has reached 1 million [7]. The increasing number of EVs will bring new opportunities to FR of power system.

There are three ways for EVs participating in FR. The first way is the localized decision-making, for which, each charger determines how much charging/discharging power is based on local information, such as load fluctuations, the arrival time of each EV and the local frequency information [8], [9]. The second way is the decentralized decision-making. In this case, the FR signals are sent to the aggregators by control center for controlling each charging device based on the operating voltage, power loss and so on [6], [10], [11]. The last way is the centralized decision-making. With the support of the communication system, the chargers are controlled by the control center [7], [12].

In the current literature, there are different optimization objectives for EVs participating in FR such as reducing frequency deviation (FD), improving FR revenue and EV owners' satisfaction [13]–[18]. In order to reduce the FD,

the coordinated control strategies of different FR resources are proposed and have better performance [19], [20]. This is because these strategies can utilize the complementarity of different FR resources efficiently. When an operation power system is safe enough, the FR revenue could be improved. The charging/discharging time of EVs could be optimized, for example, EVs charge/discharge from/to grid when the electricity price is low/high [20]–[22]. FR cost reduction, such as reducing the battery degradation cost, also could improve FR revenue [9], [23]. From the EV owners' point of view, their driving requirements are important and should be satisfied. Therefore, the state-of-charge (SOC) of EV batteries is necessary to be maximized [24], [25].

The PSOSs could be divided into five states based on the security level [26]–[28]. The optimization objectives of power system depend on the PSOS [29]–[31]. For different optimization objectives, the utilization of each FR resource is different. This is because some characteristics of resources are complementary. For example, the response speed of EVs could reach the millisecond level, the thermal power generators and hydroelectric generators just could reach the seconds level. The response speed of EVs is much faster, but the FR cost of them is higher. In our previous research in [13], the response priorities for EVs participating in FR under different PSOSs are involved. EVs participate in FR under different PSOSs is investigated, but the optimal model is not yet established.

In this paper, an optimal coordinated method for EVs participating in FR under different PSOSs is proposed. In the proposed methodology, the FR power of EVs and generators is coordinated with different optimization objectives for power system secure and economic operations. When a power system operates in normal state, the minimum FR cost is used as an optimization objective considering the battery degradation cost. In the abnormal state, the minimum frequency restoring time is considered in the optimization objective. In simulation, a series of random load and step load are added in the normal state and abnormal state respectively. Based on the proposed optimization method, the coordinated control rule between EVs and generators is drawn. The remainder of this paper is arranged as follows. The optimized model is established in Section II. The particle swarm optimization algorithm and the fuzzy set theory are employed to resolve the optimal model in Section III. In Section IV, the proposed coordinated control strategy between EVs and generators is validated. In Section V, the conclusion is made.

II. PROBLEM FORMULATION

An operation power system should maintain balance between generation and load. Any generation-load mismatch will result in FD. When the system operates in a relatively safe state, the FD is within a certain small range. As the operation power system is divided five states, only normal state is considered relatively safe [27]–[29]. In this paper, the normal state is classified as normal state, and the others are classified as abnormal state.

A. OBJECTIVE FUNCTION

The formulas on FD is adopted from [6] and [30], as shown in (1).

$$\Delta\dot{f} = \frac{1}{M}\left(\Delta P_{V2G} + \Delta P_{FRR} - \Delta P_L - D\Delta f\right) \quad (1)$$

$$\Delta P_{V2G} = \sum_{i=1}^{N} \Delta P_{EV,i} \quad (2)$$

where Δ denotes the deviation from the initial steady state; f is the system frequency; M is the angular momentum; P_{V2G} is the aggregated V2G power of all EVs; P_{FRR} is the output power of other FR resources; P_L is the frequency nonsensitive load power; D is the load-damping coefficient; $P_{EV,i}$ is the V2G power of the ith EV; N is the number of the EVs. In this paper, the EVs are assumed stay in the charging station for the most of time every day. The number of EVs participating in FR could be ensured through incentive measures or policies such as economic incentive. It is similar to demand response (DR). DR is often a cost effective technique that can provide the flexibility required to time shift loads either through prices or incentive policies [21].

The FR cost is formulated as follows:

$$C = C_{EV} + C_m \quad (3)$$

$$C_{EV} = C_{deg} + C_{char} + C_{loss} \quad (4)$$

where C is the FR cost; C_m is the FR cost of generators; C_{EV} is the FR cost of EVs, it consists of battery degradation cost C_{deg}, charging cost C_{char} and power loss cost C_{loss}; C_{char} is the cost for purchasing/selling the power from/to the power grid; C_{loss} is the cost for power transmission loss.

The battery degradation cost is result from the charging/discharging of EV batteries and it is calculated as (5) [12]

$$C_{deg} = \sum_{i\in I}\sum_{t\in W} \alpha P_{EV,it}^2 + \sum_{i\in I}\sum_{t=2}^{|W|} \beta \Delta P_{EV,it}^2 \quad (5)$$

where α and β are the model parameters; $P_{EV,it}$ is the charging power and $\Delta P_{EV,it}$ is the charging power fluctuation of the ith EV in interval t; W is the interval set; I is the set of EVs; $P_{EV,it}$ and $\Delta P_{EV,it}$ could affect battery temperature and active material of battery, they will result in more battery degradation cost.

When a power system operates in a relatively safe state, the FR cost can be considered to reduce. The objective function is shown as follows:

$$\begin{cases} \min\left\{\Delta f_{\max}, \Delta f_{aver}, C\right\}, & S_{tate} = 0 \\ \min\left\{\Delta f_{\max}, \Delta f_{aver}, t_F\right\}, & S_{tate} = 1 \end{cases} \quad (6)$$

where $\Delta f_{\max}$ and Δf_{aver} are the maximum and the average FD values during FR process, respectively; t_F is the time that the FD restores to normal range; S_{tate} is the PSOS, when the system operates in normal state it equals 0, otherwise it equals 1.

B. FR CHARACTERISTICS

1) DYNAMIC CHARACTERISTICS

The dynamic characteristics of generators mainly depend on the time constants of inlet steam chest, reheater and governor. The dynamic characteristics of EVs mainly depend on time constant of battery power adjustment (it can reach up to tens of milliseconds [6], [33]). The response speed and FR accuracy advantages will be obvious if the number of EVs is sufficient. Otherwise the output power of EVs will be restricted by capacity constraint. The output power of the generator is restricted by response speed and ramp rate, compared with that of EVs.

2) COST CHARACTERISTIC

The FR cost of EVs includes battery degradation cost, charging cost and power loss cost. The charging cost is affected by electricity price and charging power, which is expressed as (7). It is a positive number when EVs are charging and a negative number when EVs are discharging. In this paper, the charging power and discharging power which are provided for FR, are assumed to be equal. If the electricity price for purchasing and selling are also assumed to be equal, the charging cost will be zero. Therefore, the charging cost is not considered in this paper. The power loss cost results from transmission loss and is reflected in charging/discharging efficiency, which is shown in (14) and (15).

$$C_{EVch\arg e} = \sum_{i\in I}\sum_{t\in W}\left(P_{ch\arg e,it} z_{purchase,t} - P_{disch\arg e,it} z_{sell,t}\right) \tag{7}$$

where $P_{charge,it}$ and $P_{discharge,it}$ are the charging power and discharging power of the ith EV in interval t respectively; $Z_{purchase,t}$ and $Z_{sell,t}$ are the electricity price for purchasing power from grid and selling power to grid in interval t respectively.

EV battery has limited cycle life because of the fading of active materials caused by the charging and discharging cycles [36]. This cycle aging is caused by the growth of cracks in the active materials, a process similar to fatigue in materials subjected to cyclic mechanical loading [36], [37]. The influence factors can be summarized as ambient temperature, cycle depth, charging/discharging power and so on. In [12], [36], and [39], the variable of battery degradation cost equations is V2G power. It could be presumed that the equations are established for the ideal operating conditions (for example, the ambient temperature is 25 °C). The relationships between battery degradation cost and V2G power are shown in Fig. 1. The Model 1, Model 2 and Model 3 are battery degradation costs which are calculated based on [12], [36], and [38], respectively. In Model 2, the cost function is a piecewise function, the V2G power in each segment is random. In Model 3, the correlation parameters are the average values. In order to simplify the cost calculation, the cost equation of Model 1 is applied in this paper.

The battery degradation cost, which is shown as (5), is related to the total and the fluctuation of output power

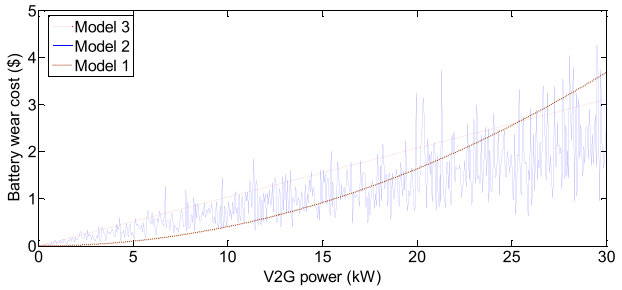

FIGURE 1. The battery degradation cost of EVs.

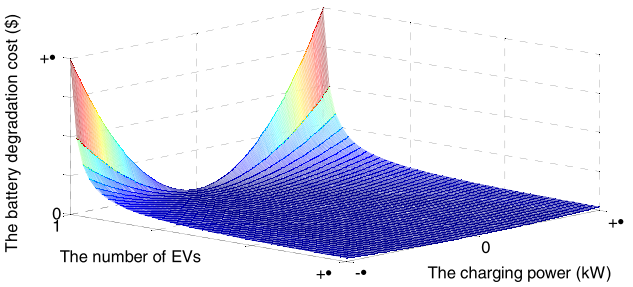

FIGURE 2. Surface chart of battery degradation cost.

of EVs during t. Over-charging/discharging or over-frequent charging/discharging will shorten service life of the battery. The battery degradation cost is illustrated in Fig. 2, in which charging power indicates FR power of EVs within time t. It can be seen that the more EVs participate in FR, the lower battery degradation cost is. In Fig. 2, battery capacity limit is not considered, and it is assumed that the charging power of each EV is the same no matter how many EVs participate in FR.

FR cost of generators is shown in (8) [32].

$$\begin{aligned} C_m &= \sum_{g=g_s}^{g_e}\sum_{t=t_s}^{t_e} C_{gt} + \sum_{g=g_s}^{g_e}\sum_{t=t_s}^{t_e} q_{pr,gt} r_{pr,gt} \\ &= \sum_{g=g_s}^{g_e}\sum_{t=t_s}^{t_e}\left[u_{gt} C_{fix,gt} + a_g G_{gt} + \frac{1}{2} b_g \left(G_{gt}\right)^2\right] \\ &\quad + \sum_{g=g_s}^{g_e}\sum_{t=t_s}^{t_e} q_{pr,gt} r_{pr,gt} \end{aligned} \tag{8}$$

where C_{gt} is the running generation cost of the gth generator during time period t; t_s is the start time of the generator participating in FR; t_e is the end time of the generator participating in FR; u_{gt} equals to 1 if the gth generator is on during time period t and to 0 if not; $C_{fix,gt}$ is the gth generator fixed generation cost during t; a_g and b_g are the generation cost parameters; G_{gt} is scheduled generation of the gth generator in the pre-contingency state during t; $q_{pr,gt}$ is the gth generator primary reserve rate during t; $r_{pr,gt}$ is scheduled primary reserve of the gth generator during t. As can be seen from (8), FR cost of generators is related to output power, generator number and reserve capacity.

C. CONSTRAINTS

1) SOCs of EVs

When EVs participate in FR, the SOC should be considered. It affects the charging/discharging capacity of each EV.

$$SOC_{\min} \le SOC_{ini,i} \le SOC_{\max} \tag{9}$$

$$E_{c,i} = \left(SOC_{\max} - SOC_{ini,i}\right) E_{0,i} \tag{10}$$

$$E_{d,i} = \left(SOC_{ini,i} - SOC_{\min}\right) E_{0,i} \tag{11}$$

where SOC_{max} and SOC_{min} are the maximum and minimum SOC of the EVs respectively; These settings are used for avoiding the batteries over-charging/discharging; $SOC_{ini,i}$ is the initial SOC of the ith EV; $E_{c,i}$ is the energy of the ith EV for charging; $E_{d,i}$ is the energy of the ith EV for discharging; $E_{0,i}$ is the rated capacity of the ith EV battery.

2) GENERATOR POWER OUTPUT

In order to avoid the output power of generators is too large or too small, the constraint is shown as (12).

$$\Delta P_{\min m,g} \le \Delta P_{m,g} \le \Delta P_{\max m,g} \tag{12}$$

where $\Delta P_{\min m,g}$ is the minimum output power of the gth generator participating in FR and $\Delta P_{\max m,g}$ is the maximum output power of the gth generator.

3) EV CHARGING/DISCHARGING POWER

As the output power of generators, the constraints for output power of EVs can be expressed as follows:

$$\Delta P_{\max D,i} \le \Delta P_{V2G,i} \le \Delta P_{\max C,i} \tag{13}$$

$$\Delta P_{V2GD,i} = \kappa \cdot K_{i,k}^{Down} \cdot \Delta P'_{V2GD,i} \tag{14}$$

$$\Delta P_{V2GC,i} = \zeta \cdot K_{i,k}^{Up} \cdot \Delta P'_{V2GC,i} \tag{15}$$

$$P_{sti,down} \le \sum_{i=1}^{N_{EV}} \Delta P_{V2G,i} \le P_{sti,up} \tag{16}$$

where $\Delta P_{\max D,i}$ is the maximum discharging power of the ith EV during time period t; $\Delta P_{\max C,i}$ is the maximum charging power of the ith EV during time period t; $\Delta P_{V2GD,i}$ and $\Delta P_{V2GC,i}$ are actual discharging power and charging power of the ith EV; ζ and κ are the transmission loss efficiency coefficients. They are both less than 1. $K_{i,k}^{Down}$ and $K_{i,k}^{Up}$ are the discharging efficiency and charging efficiency coefficients, respectively; $\Delta P'_{V2GD,i}$ and $\Delta P'_{V2GC,i}$ are the discharging and charging power of the ith EV; $P_{sti,down}$ and $P_{sti,up}$ are the lower and upper limit capacity of the stith charging station, respectively. N_{EV} is the number of EVs stay in charging station. $\Delta P'_{V2GD,i}$ and $\Delta P'_{V2GC,i}$ are vary with the SOC of the ith EV, which is formulated as (17) - (20) and shown as Fig.3 [14].

$$\begin{cases} K_{i,k}^{Down} = 1 \\ K_{i,k}^{Up} = 0 \end{cases}, \quad SOC_{i,k} \le SOC_i^{\min} \tag{17}$$

$$\begin{cases} K_{i,k}^{Down} = 0 \\ K_{i,k}^{Up} = 1 \end{cases}, \quad SOC_{i,k} \ge SOC_i^{\max} \tag{18}$$

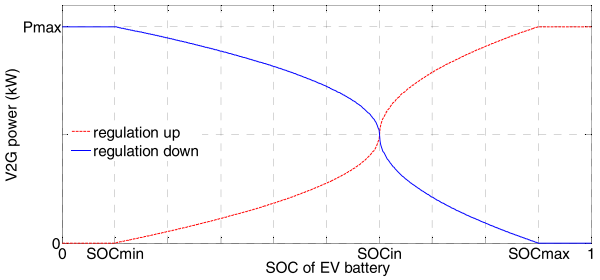

FIGURE 3. The output powers for different SOC EVs.

$$\begin{cases} K_{i,k}^{Down} = \frac{1}{2}\left(1 + \sqrt{\frac{SOC_{i,k} - SOC_i^{in}}{SOC_i^{\min} - SOC_i^{in}}}\right) \\ K_{i,k}^{Up} = \frac{1}{2}\left(1 - \sqrt{\frac{SOC_{i,k} - SOC_i^{in}}{SOC_i^{\min} - SOC_i^{in}}}\right) \end{cases}, \quad SOC_i^{\min} \le SOC_{i,k} \le SOC_i^{in} \tag{19}$$

$$\begin{cases} K_{i,k}^{Down} = \frac{1}{2}\left(1 - \sqrt{\frac{SOC_{i,k} - SOC_i^{in}}{SOC_i^{\max} - SOC_i^{in}}}\right) \\ K_{i,k}^{Up} = \frac{1}{2}\left(1 + \sqrt{\frac{SOC_{i,k} - SOC_i^{in}}{SOC_i^{\max} - SOC_i^{in}}}\right) \end{cases}, \quad SOC_i^{in} \le SOC_{i,k} \le SOC_i^{\max} \tag{20}$$

where $SOC_i^{\max}$ is the maximum SOC of the ith EV; $SOC_i^{\min}$ is the minimum SOC of the ith EV; SOC_i^{in} is the initial SOC of the ith EV at plug-in time.

III. OPTIMIZATION ALGORITHM

After the comparison among particle swarm optimization (PSO) algorithm, genetic algorithm (GA) and evolutionary algorithms (EAS), the optimization result of PSO is overall best. In this paper, the PSO algorithm is chosen. The fuzzy set theory is employed in this paper to find the best compromise solution. The solution procedures are shown as (21) and (22) [34]. The eth objective function of a solution in the set F_e is represented by a membership function μ_e. The flow chart of the optimization procedures is shown in Fig. 4.

$$\mu_e = \begin{cases} 1, & |F_e| \le |F_e|_{\min} \\ \dfrac{|F_e|_{\max} - |F_e|}{|F_e|_{\max} - |F_e|_{\min}}, & |F_e|_{\min} < |F_e| < |F_e|_{\max} \\ 0, & |F_e| \ge |F_e|_{\max} \end{cases} \tag{21}$$

$$\mu^{\theta} = \frac{\sum_{e=1}^{N_{obj}} \xi_e \mu_e^{\theta}}{\sum_{h=1}^{H} \sum_{e=1}^{N_{obj}} \xi_e \mu_e^{h}} \tag{22}$$

where $|F_e|_{\max}$ and $|F_e|_{\min}$ are the maximum and minimum value of the eth objective function respectively. For each solution θ, the normalized membership function μ_θ is calculated as (22). H is the number of solutions. The best compromise solution is the one with the maximum μ_θ. ξ_e is the weight coefficient of the eth objective function.

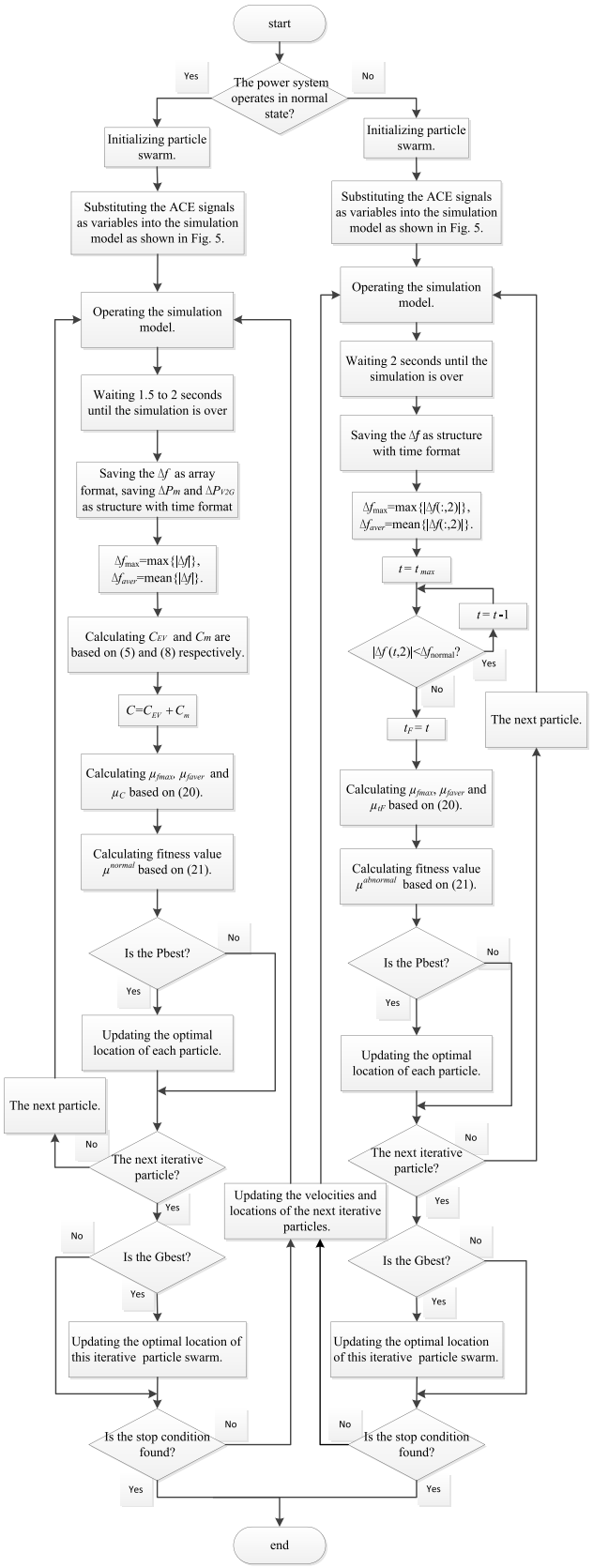

FIGURE 4. The flow chart of optimization procedures.

IV. SIMULATIONS AND RESULTS

In this paper, the proposed approach is an off-line optimization to determine the optimal coordinated control strategy for EVs and generators participating in FR. The off-line optimization process should be implemented with a great variety of load disturbances to experience enough power system scenarios in a high-accuracy simulation environment, and numerous explorations with EV charging/discharging strategies should be sampled sufficiently in various system operation states. Consequently, the optimized control strategy can then be implemented for on-site operation, and the optimal charging/discharging power for each EV can be obtained to meet the timeliness requirement based on the current system operation state.

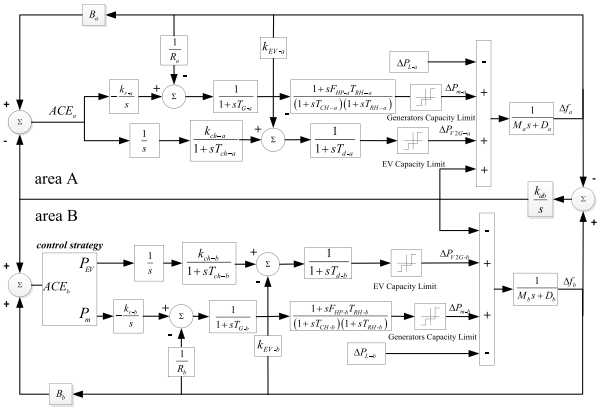

FIGURE 5. Block diagram of FR for two areas with generators and EV charging stations.

TABLE 1. Parameters of the simulation system model.

Parameters	Value	Parameters	Value
System base (MW)	10	Nominal frequency (Hz)	60
$T_{G\text{-}a}$, $T_{G\text{-}b}$ (sec)	0.5	D_a, D_b (MW/Hz)	1/6
$T_{CH\text{-}a}$, $T_{CH\text{-}b}$	0.8	R_a, R_b (Hz/MW)	0.3
$T_{RH\text{-}a}$, $T_{RH\text{-}b}$ (sec)	10	$k_{r\text{-}a}$, $k_{r\text{-}b}$ (MW/Hz/sec)	2/15
M_a, M_b (MW/Hz/s)	2.0	$F_{HP\text{-}a}$, $F_{HP\text{-}b}$	30%

The simulation model based on MATLAB/Simulink is shown as Fig. 5. The FR resources of both area A and area B include generators and EVs. The model parameters of the two-area interconnected system are taken from [6] and [13], as shown in Table I-III. The FR signal is based on the area control error (ACE) under the TBC control mode, as follows

$$ACE = \Delta P_{tie} + B\Delta f \tag{23}$$

In order to simulate the load fluctuation in normal state, a series of random load, which fluctuates within a certain range, is added in area A and area B. As the unit of the parameters in Table IV is hour, the random fluctuation time of the load in normal state is set to 1 hour. Two step loads

TABLE 2. Parameters of the EV charging station model.

Parameters	Value
EV frequency characteristic coefficient, $k_{ev\text{-}a}$, $k_{ev\text{-}b}$ (MW/Hz)	1.12
EV battery gain, $k_{ch\text{-}a}$, $k_{ch\text{-}b}$	1
EV battery filter time constant, $T_{ch\text{-}a}$, $T_{ch\text{-}b}$ (sec)	1
1st order delay of DC/AC converter, $T_{d\text{-}a}$, $T_{d\text{-}b}$ (sec)	2
The number of EVs in area A	817
The number of EVs in area B	817
The number of generators in area A	1
The number of generators in area B	1

TABLE 3. Parameters of EVs.

Parameters	Value	SOC of EVs	Number
$SOC_{\min}$	0.1	0.9	41
$SOC_{\max}$	0.9	0.8	67
SOC_{io}	0.6	0.7	90
Battery capacity (kWh)	50	0.6	270
$\Delta P_{\max D,i,}$	25	0.5	100
$\Delta P_{\max C,i}$	25	0.4	80
κ,	0.8	0.3	60
ζ	0.8	0.2	27
		0.1	32

TABLE 4. The FR cost parameters.

Parameters	Value	Parameters	Value
C_{it} ($/h)	10	Number of particles	100
a_{it} ($/MWh)	9.8	Number of iterations	100
b_{it} ($/MWh2)	0	vx mj, vx EVj	[-1.1]
$q_{pr,it}$ ($/MWh)	10	$c1$, $c2$	0.8
α ($/KWh2)	3.826×10-4	$r1$, $r2$	random[0,1]
β ($/KWh2)	7.652×10-4	ω_n, ω_{EV}	1
$\xi_{normal\text{-}fmax}$	1	$\xi_{abnormal\text{-}faverage}$	1
$\xi_{normal\text{-}faverage}$	1	$\xi_{abnormal\text{-}faverage}$	1
$\xi_{normal\text{-}cost}$	1	$\xi_{abnormal\text{-}t}$	1

are added in area A and area B respectively, for simulating the disturbed load in abnormal state of power system, one is -0.8MW the other is $P_{abnormal}$.

A. OPTIMIZATION AND ANALYSIS OF CONTROL STRATEGY

In this paper, the multiples of FR capacity allocated for EVs and generators, express as the ace signals for EVs and generators, are the decision variables. The relevant parameters are shown in Table IV [12]. The optimization objectives in different states are formulated as (6).

1) NORMAL STATE

As shown in Fig. 6 and Fig. 7, the sum of output power of EVs and generators in normal state fluctuates significantly because of the random loads. The sum output power of EVs and generators in normal state trends to increase with the increase of P_{normal}. The sum output power of EVs is small, and the output power at each moment can be negligible.

2) ABNORMAL STATE

In the abnormal state, the operation power system is not safe. In order to make the FD restore to the normal range as soon as possible, the complementary of EVs and generators should be utilized. As shown in Fig. 8 and Fig. 9, in abnormal state,

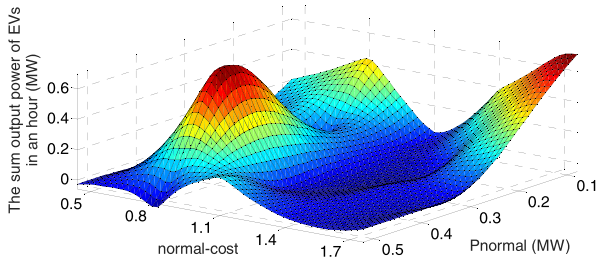

FIGURE 6. The sum output power of EVs under different scenarios in normal state.

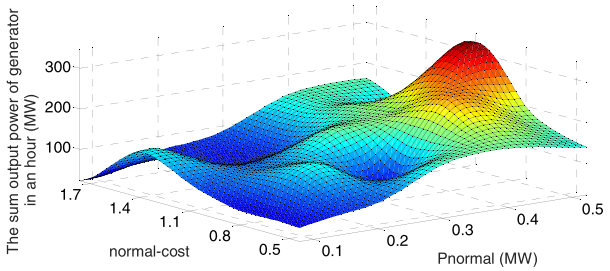

FIGURE 7. The sum output power of generators under different scenarios in normal state.

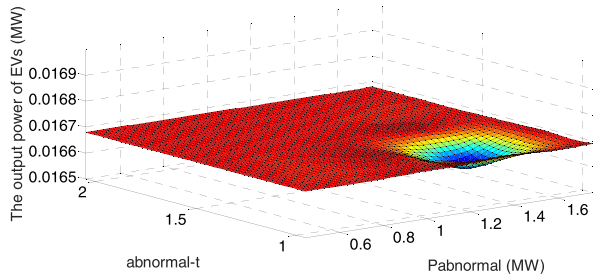

FIGURE 8. The output power of EVs under different scenarios of abnormal state.

the output power of generators increases with the increase of P_{abnormal} and the output power of EVs is always the maximum. The output power is the final stable value. In abnormal state, the optimized effect of any of these three objectives is the same, the minimum FD. Therefore, the output power has no rule with the $\xi_{\text{abnormal-t}}$.

In normal state, the output power of EVs can be negligible. In abnormal state, the output power of EVs is the maximum. The respond speed and FR accuracy of EVs, and the FR capacity of generators, are effectively utilized. The FR cost is considered.

B. SIMULATION AND DISCUSSION

The FR strategy, which is shown in area A of Fig. 5, is named STRATEGY1. As shown in [13], the FR control strategy is named STRATEGY2. In STRATEGY2, the response priorities and control strategies for the FRRs vary with different operating states. The FR control strategy optimized by the proposed optimization method, which is shown in Table 5,

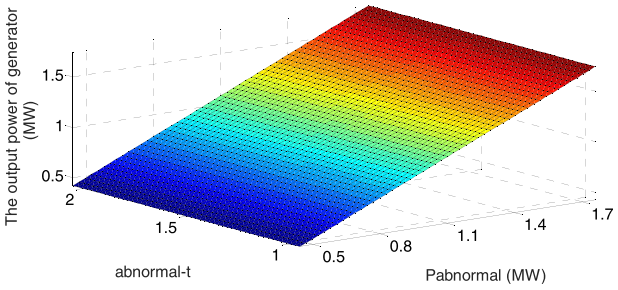

FIGURE 9. The output power of generators under different scenarios of abnormal state.

TABLE 5. The coordinated control strategy3.

	Normal state	Abnormal state
P_{EV}	0**ACE*	2**ACE*
P_{m}	0.6**ACE*	2**ACE*

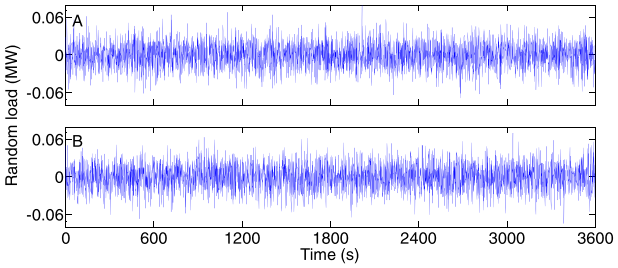

FIGURE 10. Random loads fluctuation within one hour in area A (A) and in area B (B).

is named STRATEGY3. In STRATEGY3, the number of EVs is increased to two times, is named STRATEGY3+.

In order to evaluate the effectiveness of the FR control strategies, the different indicators in different states are calculated and listed in Tables VI.

1) NORMAL STATE

The random load is assumed to be under the normal distribution [40]–[42], and it is formulated as (24) and is simulated as Fig. 10.

$$P_{random}(t) = \mu + P_{normal} \cdot \sigma \cdot randn \tag{24}$$

where P_{random} is the load fluctuation in normal state; μ and σ are parameters of the normal distribution function, they equal to 0 and 0.388. P_{normal} is the maximum value of the load fluctuation in the most of time, it equals to 0.06 MW in Fig. 10; *randn* is a standard normal distribution random number in [0,1].

The output power of different control strategies is shown in Fig. 11. In STRATEGY1 and STRATEGY2, the EVs and generators participate in FR. In STRATEGY3, only the generators undertake the FR task. In STRATEGY3, the output power of generators is the least.

Tie-line power of different control strategies is shown in Fig. 12. In STRATEGY3, the tie-line power fluctuation is

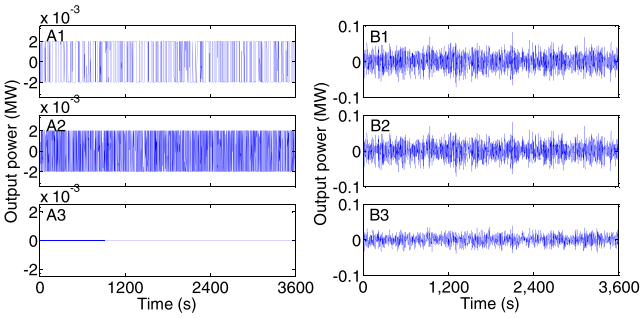

FIGURE 11. The output power of EVs with STRATEGY1 (A1), of generators with STRATEGY1 (B1), of EVs with STRATEGY2 (A2), of generators with STRATEGY2 (B2), of EVs with STRATEGY3 (A3) and of generators with STRATEGY3 (B3) in the normal state.

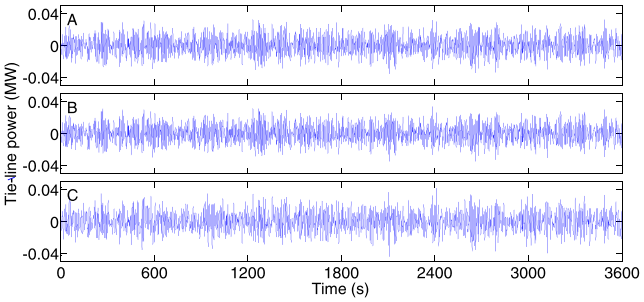

FIGURE 12. The tie-line power with STRATEGY1 (A), with STRATEGY2 (B) and with STRATEGY3 (C) in the normal state.

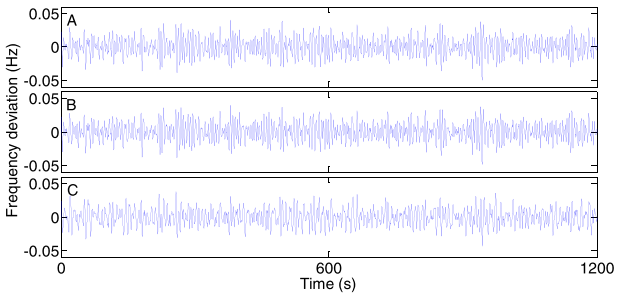

FIGURE 13. The FD with STRATEGY1 (A), with STRATEGY2 (B) and STRATEGY3 (C) in the normal state.

more dramatic than STRATEGY1 and STRATEGY2. This is because the FR power in STRATEGY3 is the least.

The FD of different coordinated control strategies is shown in Fig. 13. The FR power in STRATEGY3 is the least. However, the FD of STRATEGY3 is a little less than other strategies. As shown in Table 6, the FR effect of STRATEGY3 is the best, and the FR cost is much less than other strategies. This is because the random load fluctuates constantly. The FR cost of STRATEGY2 is less than that of STRATEGY2. This is because the output power of generators in STRATEGY3 is the less. The FR result of STRATEGY3+ is the same with STRATEGY3, this is because EVs do not participate in FR.

2) ABNORMAL STATE

A −0.8MW load and an 1.6MW load are added in area A at the 10^{th} second and area B at the 15^{th} second respectively. The output power of different strategies is shown as Fig. 14.

TABLE 6. Simulation results of different methods.

		STRATEGY1	STRATEGY2	STRATEGY3	STRATEGY3+
The normal state	The maximum FD (Hz)	0.0552	0.0542	0.0549	0.0549
	The average FD (Hz)	0.0120	0.0122	0.0106	0.0106
	The FR cost of generators ($)	276.1746	211.3497	231.0159	231.0159
	The FR cost of EVs ($)	541.3750	485.6162	0	0
	The total cost ($)	817.5496	696.9659	231.0159	231.0159
The abnormal state	The maximum FD (Hz)	0.9557	0.9552	0.9347	0.9346
	The average FD (Hz)	0.0134	0.0134	0.0096	0.0096
	The recovery time (s)	85.1717	85.1716	42.9876	42.9874

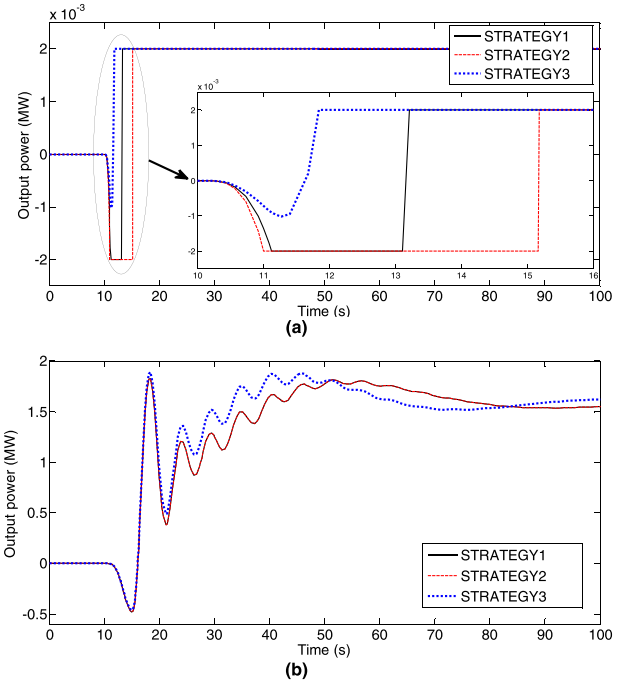

FIGURE 14. The output power of EVs (a) and generators (b) with strategies in the abnormal state.

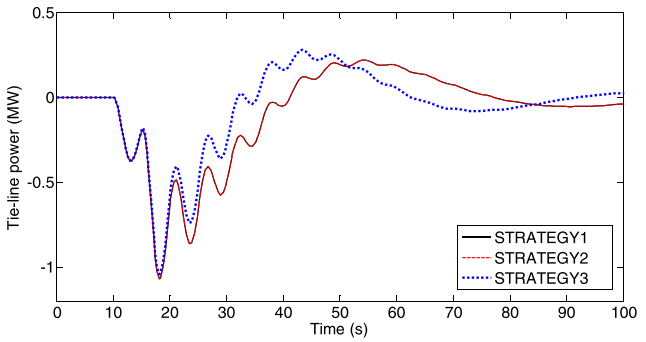

FIGURE 15. The tie-line power with strategies in the abnormal operating state.

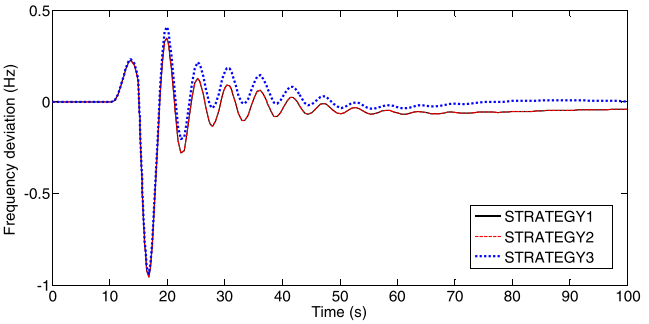

FIGURE 16. The FD with strategies in the abnormal operating state.

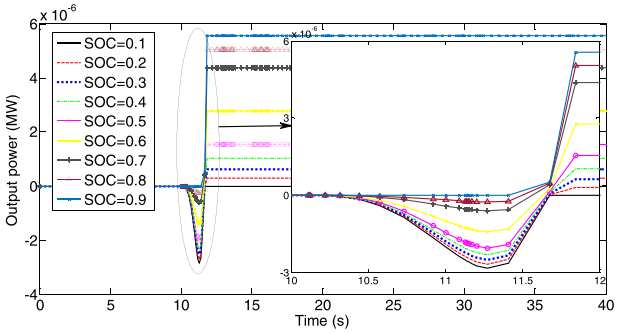

FIGURE 17. The output powers for different SOC EVs in abnormal state.

In STRATEGY2, EVs participate FR when the ACE reaches response thresholds. In STRATEGY3, the output power of EVs response faster than STRATEGY1 and STRATEGY2.

The tie-line power and FD of different strategies are shown in Fig. 15 and Fig. 16 respectively. As shown in Table 6, the performance of STRATEGY3 is the best, and the performance of STRATEGY3+ is better than STRATEGY3 because that there are more EVs participating in FR and more quick response power. The performance of STRATEGY3+ is a little better because of the capacity constraint of EVs.

In the normal state, the power system is operating in a relatively safe state and the FD fluctuates within a certain range. Therefore, the output power of FR resources could be less for FR cost reduction. In the abnormal state, the only goal is to improve system security. Therefore, the response speed and FR accuracy advantages of EVs should be utilized. Based on the optimized results, the output power of generators is appropriately less and the output power of EVs is as less as possible in normal state, and the output power of EVs is as much as possible and the remainder of the FR power is the output power of generators in abnormal state.

V. CONCLUSION

In this paper, an optimal coordinated method for EVs participating in FR under different PSOSs is proposed. In the proposed methodology, the complementarity of EVs and generators under different PSOSs is utilized. In normal state, the power system is relatively safe, while in the abnormal state, the FD must be restored to normal range as soon as possible. When a power system operates in normal state, the minimum FR cost is used as an optimization objective considering the battery degradation cost. In the abnormal state, the minimum frequency restoring time is considered in the optimization objective. In this paper, the FR cost of EVs is higher but the response speed is more rapidly. In the simulation examples, a series of random load in an hour and step load are added as disturbed loads. Based on the optimized results in different scenarios, the optimal coordinated control rule between EVs and generators is drawn. The output power of EVs and generators is suggested to be less in normal state and the output power of EVs is suggested to be more in abnormal state. The simulation results have proved that the FR cost is reduced in normal state and the frequency recovery time and the FD are improved in abnormal sate with the proposed coordinated method.

REFERENCES

[1] Y. Mu, J. Wu, J. Ekanayake, N. Jenkins, and H. Jia, "Primary frequency response from electric vehicles in the great Britain power system," *IEEE Trans. Smart Grid*, vol. 4, no. 2, pp. 1142–1150, Jun. 2013.
[2] H. Liu, J. Qi, J. Wang, P. Li, C. Li, and H. Wei, "EV dispatch control for supplementary frequency regulation considering the expectation of EV owners," *IEEE Trans. Smart Grid*, vol. 9, no. 4, pp. 3763–3772, Jul. 2018.
[3] A. F. Jensen and S. L. Mabit, "The use of electric vehicles: A case study on adding an electric car to a household," *Transp. Res. A, Policy Pract.*, vol. 106, pp. 89–99, Dec. 2017.
[4] M. H. K. Tushar, A. W. Zeineddine, and C. Assi, "Demand-side management by regulating charging and discharging of the EV, ESS, and utilizing renewable energy," *IEEE Trans. Ind. Informat.*, vol. 14, no. 1, pp. 117–126, Jan. 2018.
[5] W. Kempton and A. Dhanju, "Electric vehicles with V2G: Storage for large-scale wind power," *Windtech Int.*, vol. 2, no. 2, pp. 18–21, Mar. 2006.
[6] H. Yang, C. Y. Chung, and J. Zhao, "Application of plug-in electric vehicles to frequency regulation based on distributed signal acquisition via limited communication," *IEEE Trans. Power Syst.*, vol. 28, no. 2, pp. 1017–1026, May 2013.
[7] M. Arias, M. Kim, and S. Bae, "Prediction of electric vehicle charging-power demand in realistic urban traffic networks," *Appl. Energy*, vol. 195, pp. 738–753, Jun. 2017.
[8] S. Guner and A. Ozdemir, "Stochastic energy storage capacity model of EV parking lots," *IET Gener. Transmiss. Distrib.*, vol. 11, no. 7, pp. 1754–1761, Jun. 2017.
[9] Y. Cao *et al.*, "A cost-efficient communication framework for battery-switch-based electric vehicle charging," *IEEE Commun. Mag.*, vol. 55, no. 5, pp. 162–169, May 2017.
[10] M. Caramanis, E. Ntakou, W. W. Hogan, A. Chakrabortty, and J. Schoen, "Co-optimization of power and reserves in dynamic T&D power markets with nondispatchable renewable generation and distributed energy resources," *Proc. IEEE*, vol. 104, no. 4, pp. 807–836, Mar. 2016.
[11] K. S. Ko and D. K. Sung, "The effect of EV aggregators with time-varying delays on the stability of a load frequency control system," *IEEE Trans. Power Syst.*, vol. 33, no. 1, pp. 669–680, Jan. 2018.
[12] Y. He, B. Venkatesh, and L. Guan, "Optimal scheduling for charging and discharging of electric vehicles," *IEEE Trans. Smart Grid*, vol. 3, no. 3, pp. 1095–1105, Sep. 2012.
[13] J. Zhong *et al.*, "Coordinated control for large-scale EV charging facilities and energy storage devices participating in frequency regulation," *Appl. Energy*, vol. 123, no. 12, pp. 253–262, Jun. 2014.
[14] H. Liu, Z. Hu, Y. Song, J. Wang, and X. Xie, "Vehicle-to-grid control for supplementary frequency regulation considering charging demands," *IEEE Trans. Power Syst.*, vol. 30, no. 6, pp. 3110–3119, Nov. 2015.
[15] I. Pavić, T. Capuder, and I. Kuzle, "Value of flexible electric vehicles in providing spinning reserve services," *Appl. Energy*, vol. 157, pp. 60–74, Nov. 2015.
[16] D. T. Nguyen and L. B. Le, "Joint optimization of electric vehicle and home energy scheduling considering user comfort preference," *IEEE Trans. Smart Grid*, vol. 5, no. 1, pp. 188–199, Jan. 2014.
[17] N. DeForest, J. S. MacDonald, and D. R. Black, "Day ahead optimization of an electric vehicle fleet providing ancillary services in the Los Angeles Air Force Base vehicle-to-grid demonstration," *Appl. Energy*, vol. 210, pp. 987–1001, Jan. 2018.
[18] M. A. Kazemi, M. Sedighizadeh, M. J. Mirzaei, and O. Homaee, "Optimal siting and sizing of distribution system operator owned EV parking lots," *Appl. Energy*, vol. 179, pp. 1176–1184, Oct. 2016.
[19] Y. Lin, P. Barooah, S. Meyn and T. Middelkoop, "Experimental evaluation of frequency regulation from commercial building HVAC systems," *IEEE Trans. Smart Grid*, vol. 6, no. 2, pp. 776–783, Mar. 2015.
[20] K. W. Hu, P. H. Yi, and C. M. Liaw, "An EV SRM drive powered by battery/supercapacitor with G2V and V2H/V2G capabilities," *IEEE Trans. Ind. Electron.*, vol. 62, no. 8, pp. 4714–4727, Aug. 2015.
[21] Q. Chen *et al.*, "Dynamic price vector formation model-based automatic demand response strategy for PV-assisted EV charging stations," *IEEE Trans. Smart Grid*, vol. 8, no. 6, pp. 2903–2915, Nov. 2017.
[22] D. Dallinger, J. Link, and M. Büttner, "Smart grid agent: Plug-in electric vehicle," *IEEE Trans. Sustain. Comput.*, vol. 5, no. 3, pp. 710–717, Jul. 2014.
[23] A. O. David and I. Al-Anbagi, "EVs for frequency regulation: Cost benefit analysis in a smart grid environment," *IET Elect. Syst. Transp.*, vol. 7, no. 4, pp. 310–317, Dec. 2017.
[24] C. Peng, J. Zou, L. Lian, and L. Li, "An optimal dispatching strategy for V2G aggregator participating in supplementary frequency regulation considering EV driving demand and aggregator's benefits," *Appl. Energy*, vol. 190, pp. 591–599, Mar. 2017.
[25] T. Hoogvliet, G. Litjens, and S. Van, "Provision of regulating- and reserve power by electric vehicle owners in the Dutch market," *Appl. Energy*, vol. 190, pp. 1008–1019, Mar. 2017.
[26] L. H. Fink and K. Carlsen, "Operating under stress and strain [electrical power systems control under emergency conditions]," *IEEE Spectr.*, vol. 15, no. 3, pp. 48–53, Mar. 1978.
[27] R. Billinton and E. Khan, "A security based approach to composite power system reliability evaluation," *IEEE Trans. Power Syst.*, vol. 7, no. 1, pp. 65–71, Feb. 1992.
[28] R. J. Marceau, J. Endrenyi, R. Allan, and E. al, "Power system security assessment: A position paper," *Electra*, vol. 175, no. 2, pp. 49–77, Dec. 1997.
[29] M. K. Kim, "Multi-objective optimization operation with corrective control actions for meshed AC/DC grids including multi-terminal VSC-HVDC," *Int. J. Electr. Power Energy Syst.*, vol. 93, pp. 178–193, Dec. 2017.
[30] P. Kundur, *Power System Stability and Control*. San Francisco, CA, USA: McGraw-Hill, 1994, p. 391.
[31] A. S. O. Ogunjuyigbe, T. R. Ayodele, and O. A. Akinola, "Optimal allocation and sizing of PV/Wind/Split-diesel/Battery hybrid energy system for minimizing life cycle cost, carbon emission and dump energy of remote residential building," *Appl. Energy*, vol. 171, no. 6, pp. 153–171, Jun. 2016.
[32] J. F. Restrepo and F. D. Galiana, "Unit commitment with primary frequency regulation constraints," *IEEE Trans. Power Syst.*, vol. 20, no. 4, pp. 1836–1842, Nov. 2005.
[33] W. Kempton and J. Tomic, "Vehicle-to-grid power implementation: From stabilizing the grid to supporting large-scale renewable energy," *J. Power Sources*, vol. 144, no. 1, pp. 280–294, 2005.
[34] M. Dubarry, N. Vuillaume, and B. Y. Liaw, "From single cell model to battery pack simulation for Li-ion batteries," *J. Power Sources*, vol. 186, no. 2, pp. 500–507, Jan. 2009.
[35] D. W. Dees, V. S. Battaglia, and A. Belanger, "Electrochemical modeling of lithium polymer batteries," *J. Power Sources*, vol. 110, no. 2, pp. 310–320, Aug. 2002.
[36] B. Xu, J. Zhao, T. Zheng, E. Litvinov, and D. S. Kirschen, "Factoring the cycle aging cost of batteries participating in electricity markets," *IEEE Trans. Power Syst.*, vol. 33, no. 2, pp. 2248–2259, Mar. 2018.

[37] J. Vetter *et al.*, "Ageing mechanisms in lithium-ion batteries," *J. Power Sources*, vol. 147, nos. 1–2, pp. 269–281, 2005.
[38] H. Farzin, M. Fotuhi-Firuzabad, and M. Moeini-Aghtaie, "A practical scheme to involve degradation cost of lithium-ion batteries in vehicle-to-grid applications," *IEEE Trans. Sustain. Energy*, vol. 7, no. 4, pp. 1730–1738, Oct. 2016.
[39] M. A. Abido, "Multiobjective evolutionary algorithms for electric power dispatch problem," *IEEE Trans. Evol. Comput.*, vol. 10, no. 3, pp. 315–329, Jun. 2006.
[40] S. Zhang, H. Cheng, L. Zhang, M. Bazargan, and L. Yao, "Probabilistic evaluation of available load supply capability for distribution system," *IEEE Trans. Power Syst.*, vol. 28, no. 3, pp. 3215–3225, Aug. 2013.
[41] Z. Ren, W. Li, R. Billinton, and W. Yan, "Probabilistic power flow analysis based on the stochastic response surface method," *IEEE Trans. Power Syst.*, vol. 31, no. 3, pp. 2307–2315, May 2016.
[42] H. Liu, K. Huang, Y. Yang, H. Wei, and S. Ma, "Real-time vehicle-to-grid control for frequency regulation with high frequency regulating signal," *Protection Control Mod. Power Syst.*, vol. 3, p. 13, May 2018.
[43] S. Xia, S. Q. Bu, X. Luo, K. W. Chan, and X. Lu, "An autonomous real-time charging strategy for plug-in electric vehicles to regulate frequency of distribution system with fluctuating wind generation," *IEEE Trans. Sustain. Energy*, vol. 9, no. 2, pp. 511–524, Apr. 2018.
[44] W. Su, H. Eichi, W. Zeng, and M.-Y. Chow, "A survey on the electrification of transportation in a smart grid environment," *IEEE Trans. Ind. Informat.*, vol. 8, no. 1, pp. 1–10, Feb. 2012.

CANBING LI (M'06–SM'13) was born in Yiyang, Hunan, China, in 1979. He received the B.Sc. and Ph.D. degrees in electrical engineering from Tsinghua University, Beijing, China, in 2001 and 2006, respectively. He is currently a Professor with the College of Electrical and Information Engineering, Hunan University, Changsha, China. His research interests include smart grid, energy efficiency, and energy policy.

LONG ZENG was born in Changsha, Hunan, China, in 1987. He received the B.E. and M.S. degrees in electronic information engineering and electrical engineering from the Changsha University of Science and Technology, Changsha, in 2009 and 2013, respectively. He is currently pursuing the Ph.D. degree in electrical engineering with Hunan University, Changsha. His research interests include electric vehicles and energy efficiency.

BIN ZHOU (S'11–M'13–SM'17) was born in Hengyang, Hunan, China, in 1984. He received the B.Sc. degree in electrical engineering from Zhengzhou University, Zhengzhou, China, in 2006, the M.S. degree in electrical engineering from the South China University of Technology, Guangzhou, China, in 2009, and the Ph.D. degree from The Hong Kong Polytechnic University, Hong Kong, in 2013. He was a Research Associate and subsequently a Post-Doctoral Fellow with the Department of Electrical Engineering, The Hong Kong Polytechnic University. He is currently an Associate Professor with the College of Electrical and Information Engineering, Hunan University, Changsha, China. His main fields of research include smart grid operation and planning, renewable energy generation, and energy efficiency.

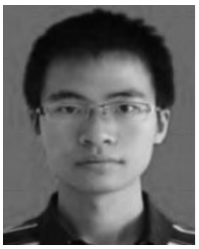

XUBIN LIU was born in Chenzhou, Hunan, China, in 1990. He received the B.E. degree in automation from the College of Electrical Engineering, Northwest University for Nationalities, Lanzhou, China, in 2013. He is currently pursuing the Ph.D. degree in electrical engineering with Hunan University, Changsha, China.

QIUWEI WU (M'08–SM'15) was born in Yixing, Jiangsu, China, in 1977. He received the B.Eng. and M.Eng. degrees in power system and its automation from the Nanjing University of Science and Technology, Nanjing, China, in 2000 and 2003, respectively, and the Ph.D. degree in power system engineering from Nanyang Technological University, Singapore, in 2009.

He was a Senior R&D Engineer with Vestas Technology R&D Singapore Pte. Ltd. from 2008 to 2009. He has been with the Department of Electrical Engineering, Technical University of Denmark, since 2009, where he held a post-doctoral position from 2009 to 2010, was an Assistant Professor from 2010 to 2013, and has been an Associate Professor since 2013. He was a Visiting Scholar with the Department of Industrial Engineering and Operations Research, University of California at Berkeley, Berkeley, in 2012, funded by the Danish Agency for Science, Technology and Innovation, Denmark. He was a Visiting Professor named by Y. Xue, an Academician of the Chinese Academy of Engineering, Shandong University, China, from 2015 to 2017. He is currently a Visiting Scholar with the School of Engineering and Applied Science, Harvard University.

His research area is power system operation and control with high renewables, including wind power modeling and control, active distribution networks, and integrated energy systems. He is an Editor of the IEEE TRANSACTIONS ON SMART GRID and the IEEE POWER ENGINEERING LETTERS. He is also an Associate Editor of the *International Journal of Electrical Power and Energy Systems*, the *Journal of Modern Power Systems and Clean Energy*, and *IET Renewable Power Generation*.

DI ZHANG (S'18) was born in Nanyang, Henan, China, in 1992. She received the B.E. degree in electric engineering and automation from the College of Physics and Electronic Engineering, Henan Normal University, Xinxiang, China, in 2014. She is currently pursuing the Ph.D. degree in electrical engineering with Hunan University, Changsha, China. Her major research interests include power system operation and control and cyber security for smart grid.

SHENG HUANG was born in Yiyang, Hunan, China, in 1988. He received the M.Sc. and Ph.D. degrees in electrical engineering from Hunan University, Changsha, China, in 2012 and 2016, respectively. He currently holds a post-doctoral position with the Center for Electric and Energy, Department of Electrical Engineering, Technical University of Denmark, Kongens Lyngby, Denmark. His research interests include renewable power generation, multi-terminal HVDC control, and wind hphantom farms control